A&A 489, 1369–1376 (2008)
DOI: 10.1051/0004-6361:200810197

Astronomy & Astrophysics

Atomic data from the IRON project

LXVI. Electron impact excitation of Fe^{18+} ⋆

K. Butler[1] and N. R. Badnell[2]

[1] Institut für Astronomie und Astrophysik, Scheinerstr. 1, 81679 München, Germany
e-mail: butler@usm.uni-muenchen.de
[2] Department of Physics, University of Strathclyde, Glasgow G4 0NG, UK
e-mail: badnell@phys.strath.ac.uk

Received 14 May 2008 / Accepted 15 July 2008

ABSTRACT

Context. Accurate electron collisional data are required for the analysis of the Fe XIX astrophysical spectrum, in particular in the sun. Such an analysis can provide information on the physical characteristics of the coronal plasma.
Aims. An extensive target is used in an R-matrix scattering calculation to provide the necessary data for Fe^{18+}. The use of the R-matrix method includes the resonance contribution lacking in the distorted wave approach and the large target improves the accuracy of the close-coupling approximation.
Methods. The R-Matrix package described by Berrington et al. (1995, Comput. Phys. Commun., 92, 290) as provided by the UK RmaX project has been used to calculate electron collisional data among 342 levels of Fe^{18+}. We have used the intermediate-coupling frame-transformation (ICFT) method (Griffin et al. 1998, J. Phys. B: At. Mol. Opt. Phys., 31, 3713) to transform data obtained in a 166 term LS-coupling calculation. Contributions from the mass and Darwin interactions have also been included in the Hamiltonian.
Results. Collision stengths for all transitions between the 342 levels of Fe^{18+} are presented. They are tabulated over a wide range of electron temperatures of astrophysical interest. The results are compared with the earlier Iron Project work of Butler & Zeippen (2001, A&A, 372, 1083) and also with that of McLaughlin et al. (2001, J. Phys. B: At. Mol. Opt. Phys., 34, 4521) and Landi & Gu (2006, ApJ, 640, 1171). The agreement is reasonable for the low-lying transitions. Larger differences are found for the more highly excited states.

Key words. atomic data – atomic processes – plasmas

1. Introduction

Accurate atomic data for highly ionized ions of iron are essential for the interpretation of the the X-ray spectrum in hot plasmas. X-ray observations of the solar corona, e.g. Wang et al. (2006) and the launch of the Chandra and XMM-Newton satellites have increased the need for such data.

The Iron Project (Hummer et al. 1993) was called into life to meet the need for such data and the project has published a large number of papers providing results for most of the ions of Iron. In particular, Butler & Zeippen (BZ, 2001) published collisional data for the O-like ion of iron Fe XIX. These were calculated in a Breit-Pauli R-matrix approximation in which transitions among 92 levels of the $n = 2$ and $n = 3$ complexes were considered. At the same time, McLaughlin et al. (2001) published a similar, but smaller, calculation for the same ion. Very recently Landi & Gu (2006) have produced a large amount of radiative and collisional data for ions of Fe XVII–XXII using the Flexible Atomic Code (FAC, Gu 2003). The collisional data in this case were obtained in the distorted wave approximation with a target based on single-electron orbitals obtained from the Dirac equations. They included levels $n \leq 5$ in their target but resonance contributions only for $n \leq 3$ from the work of Gu (2003) were added in the independent-process, isolated-resonance approximation. Landi & Gu (2006) provided data for 630 levels of Fe XIX and also pointed out some deficiencies in a few of the transitions of BZ, which showed jumps or problems in the high energy behaviour of the collision strength. The earlier work on this ion of Loulergue et al. (1985), Bhatia et al. (1989) and Zhang & Sampson (2001) has been discussed in detail by BZ. The discussion will not be repeated here.

The use of the Breit-Pauli R-matrix method restricts the number of levels that can be included in the target since the Hamiltonian matrices can become very large. Thus, Griffin et al. (1998) developed the ICFT (intermediate coupling frame transformation) method which includes the relativistic effects via, as the name suggests, a frame transformation. The most time-consuming parts of the calculations can then be carried out in LS-coupling leading either to a much smaller problem or allowing many more target levels to be included. Thus it was decided to extend the BZ calculation to include the $n = 4$ levels using the ICFT technique.

In the following section we give an overview of the calculation, in particular the target is specified and its quality is assessed, while in Sect. 3 we compare the present results with those of earlier calculations, particularly those of BZ and Landi & Gu. A brief final summary is given in Sect. 4.

2. Method

The present results were obtained using the techniques and programs developed by the Iron/RmaX projects

⋆ Full Table 4 is only available in electronic form at the CDS via anonymous ftp to cdsarc.u-strasbg.fr (130.79.128.5) or via http://cdsweb.u-strasbg.fr/cgi-bin/qcat?J/A+A/489/1369

Table 1. Configurations used in the CI expansion. Those above the line comprise the target.

$2s^22p^4$	$2s2p^5$	$2p^6$	
$2s^22p^33s$	$2s^22p^33p$	$2s^22p^33d$	
$2s2p^43s$	$2s2p^43p$	$2s2p^43d$	
$2p^53s$	$2p^53p$	$2p^53d$	
$2s^22p^34s$	$2s^22p^34p$	$2s^22p^34d$	$2s^22p^34f$
$2s2p^44s$	$2s2p^44p$	$2s2p^44d$	$2s2p^44f$
$2p^54s$	$2p^54p$	$2p^54d$	$2p^54f$

Table 2. The λ parameters for Fe XIX.

$n\ell$	$\lambda_{n\ell}$	$n\ell$	$\lambda_{n\ell}$
1s	1.40116	4s	1.17077
2s	1.27330	4p	1.12115
2p	1.20277	4d	1.16054
3s	1.17354	4f	1.18512
3p	1.12012		
3d	1.16378		

(Hummer et al. 1993) and parallel closely the methodology used by Badnell & Griffin (2001) on the C-like ion of iron Fe XXI. Thus we do not describe the method in detail but refer the interested reader to the papers cited. We do, however, provide the information on the target and collisional calculation necessary to be able to judge the quality of the calculation. The description of the target is particularly important in this respect.

The target wavefunctions were obtained in the configuration interaction approximation using AUTOSTRUCTURE (Badnell 1986) which is based on the SUPERSTRUCTURE program of Eissner et al. (1974). The expansion comprises 24 configurations as listed in Table 1. The orbitals have been computed in a Thomas-Fermi-Dirac-Almadi potential and the lambda parameters used are to be found in Table 2. These have been determined by optimizing the sum of the energies of all the 262 LS-coupling terms from all the configurations. The main difference between the target used here and that of BZ is the number of levels so that there is little difference in the quality of the agreement with the observed energy level data of Corliss & Sugar (1982). This is shown in Table 3 where only those levels with observed values are to be found. The largest errors are 3% for the $2s^22p^4\ ^1D$ and 1.4% or less for all other levels. Generally the error is well under 1%. Thus the wavefunctions reproduce the observed energies well.

A further indication of the quality of the target wavefunctions is the accuracy of the radiative data calculated from them. There are two extensive sets of oscillator strengths with which we can compare. Landi & Gu (2006) have tabulated the f-values associated with their collisional calculation in the Chianti database (Landi et al. 2006). We compare with their values in Fig. 1. The agreement with the lower levels is excellent as shown in Fig. 1a while the differences are larger when data for the higher levels is included (Fig. 1b). There is considerable mixing in the higher levels which may explain the differences. For example, the largest discrepancy involves the $2s^22p^3(^2D)3d\ ^3P_1$ state (level 72) which has the expansion

$$\begin{aligned} 2s^22p^3(^2D)3d^3P_1 \;=\; & 0.5326 \times 2s^22p^3(^2D)3d^3P_1 \\ & +0.4457 \times 2s^22p^3(^2D)3d^1P_1 \\ & +0.3470 \times 2s^22p^3(^2P)3d^1P_1 \\ & +0.3610 \times 2s^22p^3(^2D)3d^3S_1 \end{aligned}$$

so it is far from being pure. Indeed the agreement can be further improved by reassigning the levels involved but it is still the case that the levels are very sensitive to details of the configuration action treatment and can only be treated accurately with very large CI expansions (which are unsuitable for collision calculations).

The picture is similar when we compare our results with those of Kotochigova et al. (2007). They used an ab initio multiconfiguration Dirac-Fock-Sturm method combined with second order Brillouin-Wigner many-body perturbation theory and quote an accuracy of better than 1% for their oscillator strengths. We find excellent agreement with their values for the $2p^4$–$2p^33s$ transitions where the mixing is small (Fig. 2a) while there are again larger differences for the $2p^4$–$2p^33d$ lines (Fig. 2b). Indeed it proved difficult to match the two sets of f-values since they provide only wavelengths and J-values so that some of the scatter is probably due to errors in the level assignment.

There is no systematic error in any of these comparisons and the target energies are in good agreement with observation so that it is clear that the target is of good quality.

The collisional problem was solved using the R-matrix method. The inner region programs are based on the original R-matrix suite of Berrington et al., (1995) which include exchange and those of Burke et al. (1992) without exchange. The R-matrix box had a radius of 3.65 a.u. and 50 continuum waves were used in the expansion which allowed calculations up to an energy of 1000 Ryd to be made. The number of continuum functions could be reduced for the high L values in the non-exchange package without loss of accuracy. Of the 24 configurations in the CI target expansion, 16 were retained in the target expansion, $2s^22p^4$, $2s2p^5$, $2p^6$,$2s^22p^33\ell$,$2s2p^43\ell$,$2p^53\ell$ and $2s^22p^34\ell$ for all possible ℓ values. This leads to a total of 166 LS terms and 342 intermediate coupling levels. The mass and Darwin one body relativistic terms were included in the Hamiltonian.

We have not replaced the target energies with the observed values since the accuracy is high, particularly for the higher levels.

An intermediate coupling frame transformation (Griffin et al. 1998) has been used to simplify the collisional problem using the codes provided by the APAP/RmaX projects at http://amdpp.phys.strath.ac.uk/UK_APAP/. This allows LS-coupling K-matrices to be transformed to intermediate coupling values reducing the size of the Hamiltonian matrices to be treated in the collisional problem. Term-coupling coefficients, consistent with the target, have also been included in the treatment. This further increases the accuracy of the target description.

Exchange has been included for values of J up to 19/2 with J values from 21/2 to 115/2 inclusive being treated in a non-exchange approximation. The collision strengths were further "topped-up" using the Burgess sum-rule (Burgess 1974) for the dipole transitions and a geometric series for the non-dipole transitions (Badnell & Griffin 2001). An energy mesh of $10^{-5}\ z^2$ Ryd has been used in the resonance region $z = 19$ being the residual charge on the ion. Above the last threshold this has been reduced to $10^{-2}\ z^2$ Ryd since the collision strengths at these energies are slowly varying.

The resulting collision strengths have been convolved with a Maxwellian distribution to produce the temperature dependent effective collision strengths on a grid of ten energies. An appropriate infinite energy point, again consistent with the target description, has been generated using AUTOSTRUCTURE (see Whiteford et al. 2001) allowing the high temperature collision rates to be determined accurately. This also allows the rates to be interpolated smoothly. The entire data set, energy levels,

Table 3. Comparison of calculated and observed energies (Sugar & Corliss 1985). The index refers to the energy order in the full list.

Index	Level designation			E_{calc} (cm^{-1})	E_{obs} (cm^{-1})	% Diff.	Index	Level designation			E_{calc} (cm^{-1})	E_{obs} (cm^{-1})	% Diff.
1	$2s^22p^4$	^{3}P	2.0	0.	0.	0.0	72	$2s^22p^3$3d	^{3}P	1.0	7 425 337.	7 403 660.	0.3
2	$2s^22p^4$	^{3}P	0.0	74 379.	75 250.	−1.2	74	$2s^22p^3$3d	^{3}S	1.0	7 446 709.	7 431 778.	0.2
3	$2s^22p^4$	^{3}P	1.0	89 465.	89 441.	0.0	75	$2s2p^4$3s	^{5}P	2.0	7 461 916.	7 446 192.	0.2
4	$2s^22p^4$	^{1}D	2.0	173 789.	168 852.	2.9	78	$2s^22p^3$3d	^{3}F	3.0	7 484 397.	7 456 951.	0.4
5	$2s^22p^4$	^{1}S	0.0	328 622.	325 140.	1.1	81	$2s2p^4$3s	^{3}P	2.0	7 515 718.	7 503 567.	0.2
6	$2s2p^5$	^{3}P	2.0	931 202.	922 890.	0.9	83	$2s^22p^3$3d	^{3}F	4.0	7 523 032.	7 498 377.	0.3
7	$2s2p^5$	^{3}P	1.0	994 247.	984 740.	1.0	87	$2s^22p^3$3d	^{3}D	3.0	7 560 813.	7 544 892.	0.2
8	$2s2p^5$	^{3}P	0.0	1 039 753.	1 030 020.	0.9	91	$2s2p^4$3s	^{3}P	0.0	7 586 327.	7 572 355.	0.2
9	$2s2p^5$	^{1}P	1.0	1 285 054.	1 267 600.	1.4	93	$2s2p^4$3p	^{5}P	3.0	7 644 686.	7 638 836.	0.1
10	$2p^6$	^{1}S	0.0	2 164 551.	2 134 180.	1.4	94	$2s2p^4$3p	^{5}P	2.0	7 645 595.	7 638 836.	0.1
11	$2s^22p^3$3s	^{5}S	2.0	6 643 982.	6 630 860.	0.2	97	$2s2p^4$3p	^{3}D	3.0	7 691 047.	7 681 672.	0.1
12	$2s^22p^3$3s	^{3}S	1.0	6 697 283.	6 670 224.	0.4	100	$2s2p^4$3s	^{3}D	2.0	7 729 578.	7 710 594.	0.2
13	$2s^22p^3$3s	^{3}D	2.0	6 801 081.	6 785 134.	0.2	104	$2s2p^4$3p	^{3}S	1.0	7 741 818.	7 737 543.	0.1
14	$2s^22p^3$3s	^{3}D	1.0	6 803 116.	6 786 468.	0.2	105	$2s2p^4$3p	^{5}D	3.0	7 744 165.	7 737 543.	0.1
15	$2s^22p^3$3s	^{3}D	3.0	6 836 740.	6 817 097.	0.3	106	$2s2p^4$3p	^{3}D	2.0	7 749 930.	7 737 543.	0.2
16	$2s^22p^3$3s	^{1}D	2.0	6 856 867.	6 839 076.	0.3	108	$2s2p^4$3p	^{3}P	0.0	7 788 782.	7 758 999.	0.4
21	$2s^22p^3$3s	^{3}P	1.0	6 922 234.	6 894 706.	0.4	138	$2s2p^4$3d	^{5}F	1.0	8 033 259.	8 025 682.	0.1
25	$2s^22p^3$3s	^{3}P	2.0	6 979 570.	6 952 652.	0.4	145	$2s2p^4$3d	^{3}F	3.0	8 054 338.	8 044 363.	0.1
32	$2s^22p^3$3p	^{3}D	3.0	7 071 554.	7 042 841.	0.4	149	$2s2p^4$3d	^{3}F	2.0	8 097 896.	8 085 188.	0.2
33	$2s^22p^3$3p	^{1}F	3.0	7 092 499.	7 068 038.	0.3	152	$2s2p^4$3d	^{3}D	3.0	8 111 868.	8 097 521.	0.2
37	$2s^22p^3$3p	^{3}P	2.0	7 151 035.	7 130 244.	0.3	154	$2s2p^4$3d	^{3}P	2.0	8 130 880.	8 118 934.	0.1
42	$2s^22p^3$3d	^{5}D	0.0	7 189 143.	7 174 631.	0.2	188	$2s2p^4$3d	^{1}D	2.0	8 453 397.	8 435 474.	0.2
43	$2s^22p^3$3d	^{5}D	2.0	71 89 879.	7 174 631.	0.2	240	$2s^22p^3$4d	^{3}D	2.0	9 252 147.	9 236 115.	0.2
45	$2s^22p^3$3d	^{5}D	3.0	7 190 390.	7 174 631.	0.2	242	$2s^22p^3$4d	^{3}D	1.0	9 259 155.	9 236 061.	0.3
47	$2s^22p^3$3p	^{3}P	0.0	7 228 449.	7 224 211.	0.1	243	$2s^22p^3$4d	^{3}D	3.0	9 262 404.	9 245 562.	0.2
50	$2s^22p^3$3d	^{3}D	2.0	7 240 102.	7 223 491.	0.2	270	$2s^22p^3$4d	^{3}F	2.0	9 369 667.	9 344 416.	0.3
53	$2s^22p^3$3d	^{3}D	1.0	7 265 451.	7 250 810.	0.2	276	$2s^22p^3$4d	^{3}F	3.0	9 377 085.	9 359 790.	0.2
54	$2s^22p^3$3d	^{3}D	3.0	7 266 781.	7 246 902.	0.3	279	$2s^22p^3$4d	^{3}D	2.0	9 390 306.	9 383 121.	0.1
56	$2s^22p^3$3d	^{3}F	2.0	7 332 268.	7 313 503.	0.3	280	$2s^22p^3$4d	^{3}P	1.0	9 395 432.	9 383 121.	0.1
57	$2s^22p^3$3d	^{3}F	3.0	7 345 403.	7 327 081.	0.3	285	$2s^22p^3$4d	^{3}G	5.0	9 413 508.	9 385 265.	0.3
59	$2s^22p^3$3d	^{3}G	3.0	7 350 985.	7 333 685.	0.2	287	$2s^22p^3$4d	^{3}P	0.0	9 420 581.	9 397 613.	0.2
61	$2s^22p^3$3d	^{3}D	1.0	7 354 808.	7 341 636.	0.2	290	$2s^22p^3$4f	^{3}G	3.0	9 432 486.	9 405 295.	0.3
66	$2s^22p^3$3d	^{3}P	2.0	7 395 236.	7 377 446.	0.2	292	$2s^22p^3$4f	^{3}F	4.0	9 433 949.	9 405 021.	0.3
67	$2s^22p^3$3d	^{3}P	1.0	7 403 505.	7 377 896.	0.3	298	$2s^22p^3$4d	^{1}D	2.0	9 437 703.	9 423 827.	0.1
68	$2s2p^4$3s	^{5}P	3.0	7 413 683.	7 393 777.	0.3	322	$2s^22p^3$4d	^{3}D	1.0	9 507 979.	9 480 818.	0.3
71	$2s^22p^3$3d	^{3}D	2.0	7 423 782.	7 403 889.	0.3							

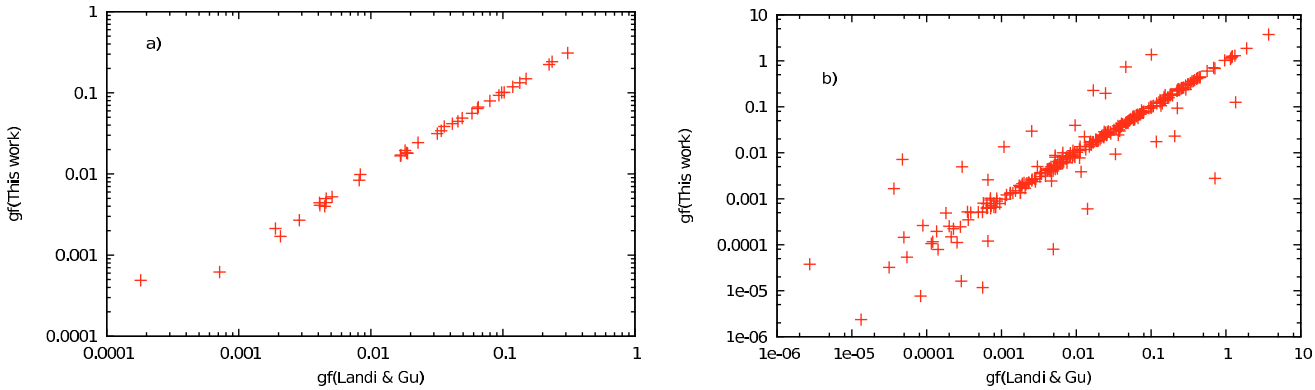

Fig. 1. Comparison of the gf-values from this work with those of Landi & Gu (2006) **a)** values with upper level index less than 45; **b)** all values.

transition probabilities and effective collision strengths is available online in the machine readable adf04 format described in the ADAS manual (Summers 2004).

3. Results

As indicated in the introduction, BZ have already compared with the earlier distorted wave results of Loulergue et al. (1985), Bhatia et al. (1989) and Zhang & Sampson (2001). The reader is referred to BZ for the details.

A small sample of the data is presented in Table 4.

We first compare the collision strengths of BZ with our own in Figs. 3–6. Overall there is good agreement between the two calculations for the lowest levels, (Figs. 3, 4) the main difference being the resonances occurring between 40 and 50 Ryd. BZ had included some of the higher lying resonances as bound states in the close-coupling expansion reducing the difference in the

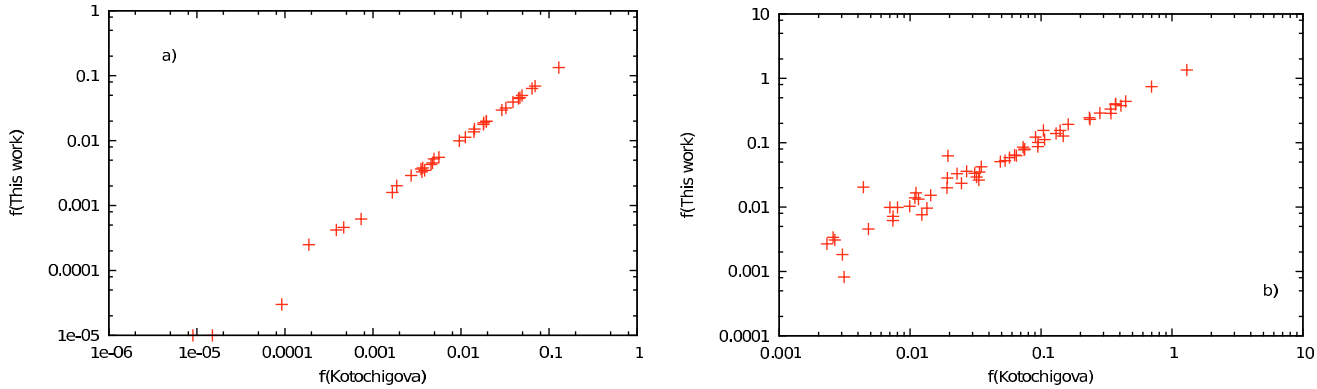

Fig. 2. Comparison of the f-values from this work with those of Kotochigova et al. (2007) **a)** transitions to 3s levels **b)** transitions to 3 d levels.

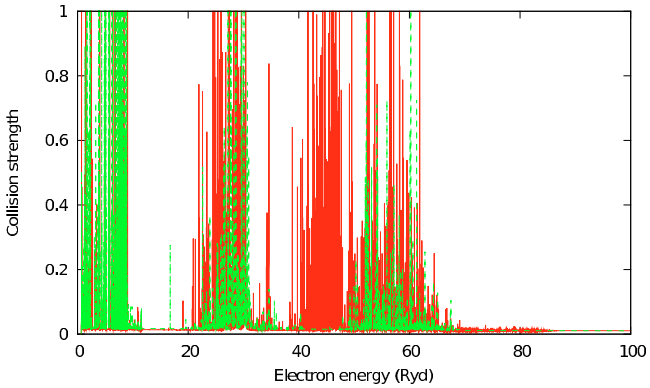

Fig. 3. Comparison of the collision strengths for the $2p^4\ ^3P_2$–$2p^4\ ^3P_0$ calculated in this work (solid line, red in the online version) with those of BZ (dashed, green).

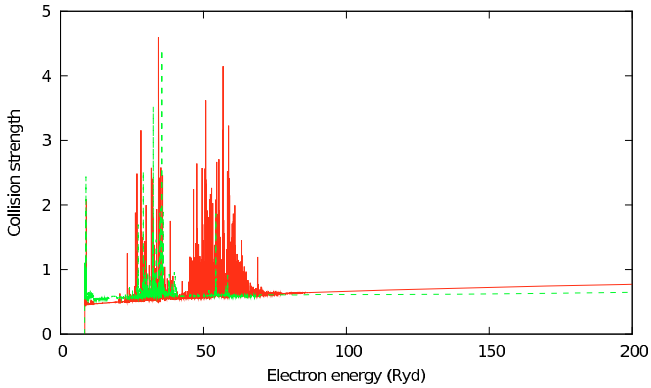

Fig. 5. Comparison of the collision strengths for the $2p^{4\,3}P_0$–$2s2p^{5\,3}P_2$ calculated in this work (solid line, red) with those of BZ (dashed, green).

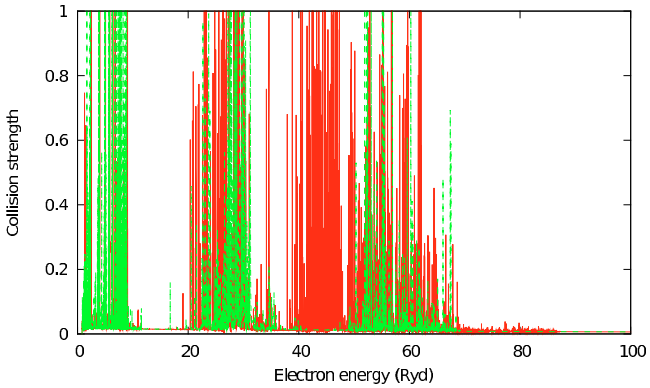

Fig. 4. Comparison of the collision strengths for the $2p^4\ ^3P_0$–$2p^4\ ^3P_1$ calculated in this work (solid line, red) with those of BZ (dashed, green).

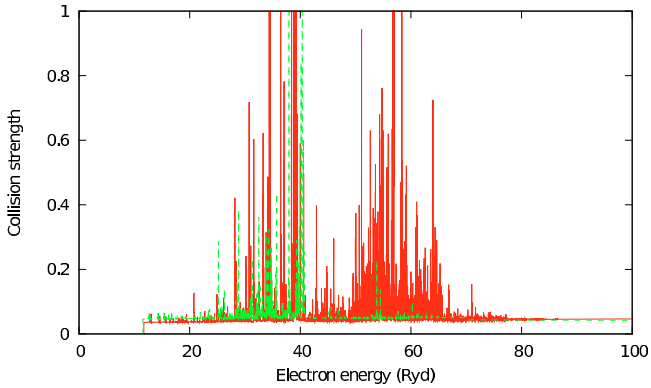

Fig. 6. Comparison of the collision strengths for the $2p^{4\,3}P_0$–$2s2p^{5\,1}P_1$ calculated in this work (solid line, red) with those of BZ (dashed, green).

60 Ryd energy region. This agreement is encouraging since the two calculations differ not only in the size of the target but in the treatment of the relativistic effects. We have used a frame transformation whereas BZ have included the spin-orbit operator directly in the inner region calculation.

Figure 5 shows an example of the top-up problem of BZ discussed by Landi & Gu (2006). At high energies the cross section does not increase with energy as it should in the BZ data. Finally, the collision strength for the $2p^{4\,3}P_0$–$2s2p^{5\,1}P_1$ transition shown in Fig. 6 is an example of a cross section to more highly lying states in which the increase in the resonant contributions to the cross section is obvious and the corresponding increase in the effective collision strength can be seen in Fig. 8b.

Of more direct interest for astrophysical purposes are the effective collision strengths, the collision strengths convolved with a Maxwellian distribution. Here we can compare not only with BZ but also with McLaughlin et al. (2001) and Landi & Gu (2006). We have obtained the Landi & Gu data from the Chianti database (Landi et al. 2006) using the Chianti software (Dere et al. 1997). There the data have been fitted to splines in a way first introduced by Burgess & Tully (1992) but only data for transitions from the lowest 4 levels are available. McLaughlin et al. (2001) have published data only for transitions among the 5 levels of the $2s^22p^4$ configuration. We begin with these transitions which are shown in Fig. 7.

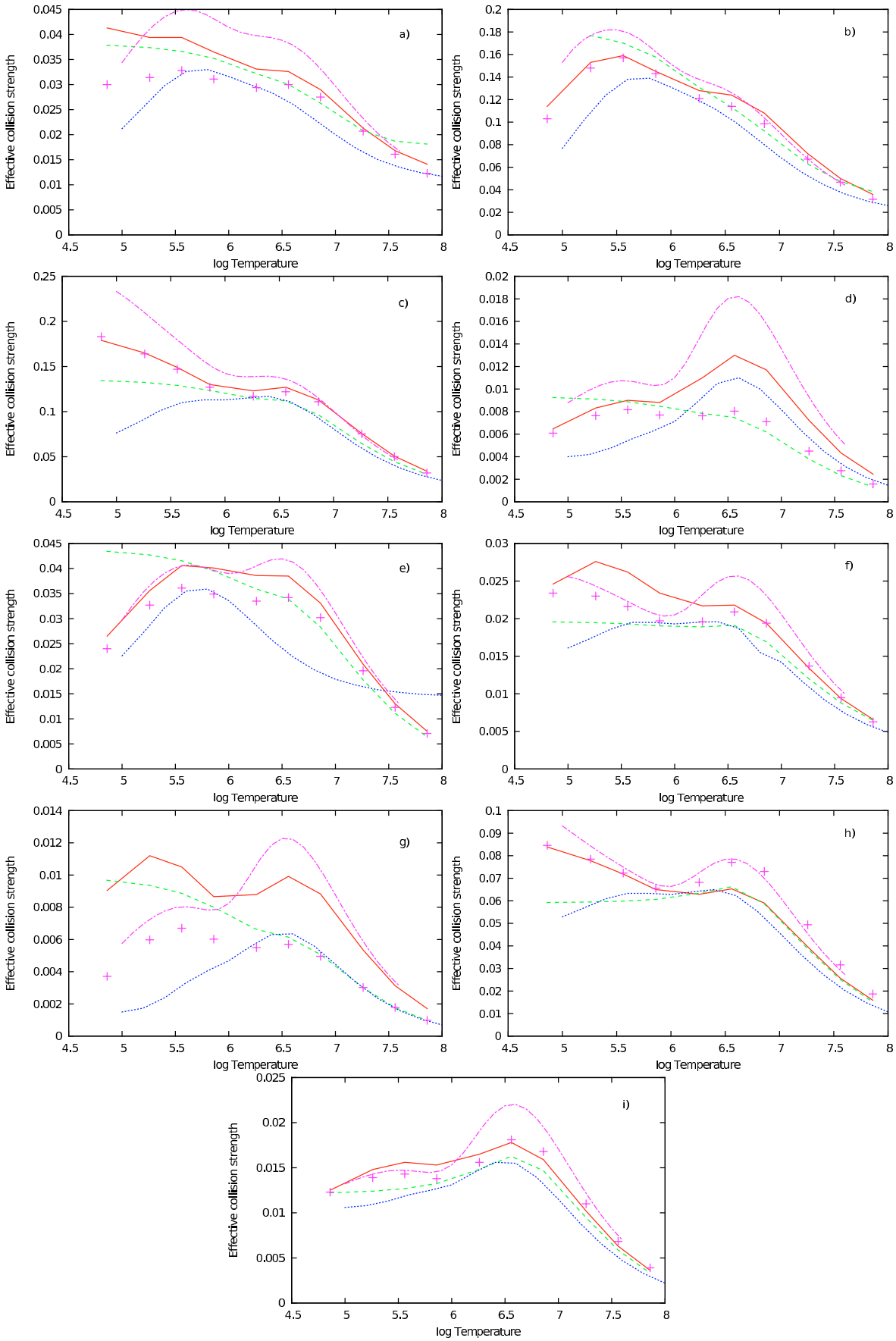

Fig. 7. Comparison of effective collision strengths for transitions among levels of the the $2s^2 2p^4$ ground configuration: this work (solid line, red in the online version), Butler & Zeippen (dashed-dotted, magenta, 2001), Landi & Gu (dashed, green, 2006), McLaughlin et al. (dotted, blue, 2001), and corrected BZ values (crosses) Transitions with level indices **a)** 1−2, **b)** 1−3, **c)** 1−4, **d)** 1−5, **e)** 2−3, **f)** 2−4, **g)** 2−5, **h)** 3−4, **i)** 3−5.

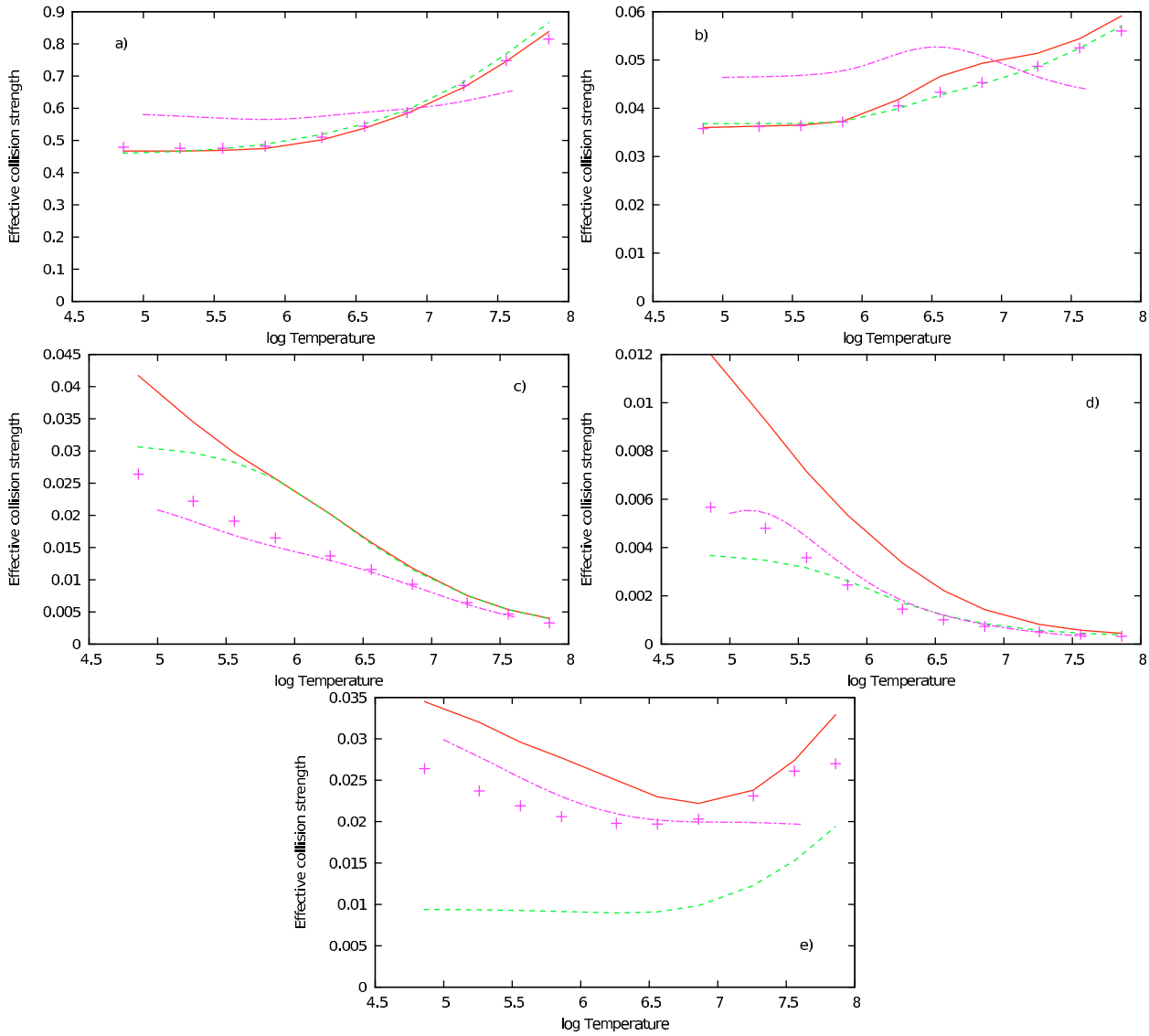

Fig. 8. Comparison of effective collision strengths from the $2s^2 2p^4 {}^3P_2$ ground level to various excited states: this work (solid line, red in the online version), Butler & Zeippen (dashed-dotted, magenta, 2001), Landi & Gu (dashed, green, 2006), corrected BZ (crosses). Transitions with level indices **a)** 1−6, **b)** 1−9, **c)** 1−45, **d)** 1−49, **e)** 1−50.

The BZ data are affected by numerical errors making an assessment of the effect of the resonances converging to $n = 4$ difficult. To alleviate this problem we have rerun their calculation using a finer energy mesh and these data are also to be found in the figures. In this way it is obvious that the discrepancies between the present work and that of BZ are, to a large part, the result of numerical problems. In the following discussion we concentrate on our corrected "BZ" values as this highlights the physics.

The agreement between the calculations at high temperatures is good on the whole, the exceptions being the high temperature behaviour of the Landi & Gu data for the 1−2 transition (Fig. 7a), which is presumably a problem with the spline fit, the McLaughlin et al. data for the 2−3 transition (Fig. 7e) and the difference between BZ/this work and Landi & Gu McLaughlin et al. for the 2−5 transition (Fig. 7g). A test calculation with the target described by McLaughlin et al. shows that there are some numerical problems in this work, possibly connected with the energy grid, and the agreement is much better than indicated in the figure. The 2−5 transition is sensitive to the resonant contribution since the background is very small (see the last column in Table 4) and thus there is a larger increase in the rate compared to the other transitions. On the other hand the rate is small and differences here will have less of an impact on line analyses.

The differences at lower temperatures are larger due to the resonance contributions as indicated in the collision strength plots. McLaughlin et al. used a much smaller target so that their cross sections are smaller in general. The differences between this work and BZ are mostly caused by the energy mesh used since BZ used a coarser mesh at intermediate energies. This means that in general, the BZ data are too large.

Note also that the effect of the resonances associated with the $n = 4$ thresholds is to increase the rates. The Landi & Gu (2006) results, which include only the $n = 3$ resonances, are generally smaller at intermediate temperatures

Effective collision strengths from the ground state to a selection of more highly excited upper states are shown in Fig. 8. The agreement with Landi & Gu is good, particularly for the higher

Table 4. Data for transitions among the $n = 2$ levels in adf04 format. In brief, an indexed list of energy levels (in cm^{-1}) is followed by the temperatures (K) and then a single line for each transition. Indices pointing to the energy levels involved are followed by a transition probability and then the effective collision strengths. The final point is the value at infinite temperature. The number $a \pm b$ is $a \times 10^{\pm b}$.

```
  FE+18        26        19      11850000.(3P)
      1        2s22p4(3P) (3)1( 2.0)              0.
      2        2s22p4(3P) (3)1( 0.0)          74379.
      3        2s22p4(3P) (3)1( 1.0)          89465.
      4        2s22p4(1D) (1)2( 2.0)         173789.
      5        2s22p4(1S) (1)0( 0.0)         328622.
      6         2s2p5(3P) (3)1( 2.0)         931202.
      7         2s2p5(3P) (3)1( 1.0)         994247.
      8         2s2p5(3P) (3)1( 0.0)        1039753.
      9         2s2p5(1P) (1)1( 1.0)        1285054.
     10           2p6(1S) (1)0( 0.0)        2164551.
     -1
  19.00     3       7.22+04 1.80+05 3.61+05 7.22+05 1.80+06 3.61+06 7.22+06 1.80+07 3.61+07 7.22+07
     2    1 0.00+00 4.13-02 3.94-02 3.94-02 3.65-02 3.31-02 3.26-02 2.90-02 2.13-02 1.68-02 1.41-02 1.14-02
     3    1 0.00+00 1.14-01 1.53-01 1.59-01 1.45-01 1.28-01 1.24-01 1.08-01 7.21-02 5.01-02 3.59-02 1.82-02
     4    1 0.00+00 1.79-01 1.65-01 1.49-01 1.30-01 1.23-01 1.27-01 1.13-01 7.57-02 5.07-02 3.39-02 1.23-02
     5    1 0.00+00 6.47-03 8.32-03 9.00-03 8.81-03 1.10-02 1.30-02 1.17-02 7.22-03 4.33-03 2.45-03 1.32-04
     6    1 3.58+10 4.67-01 4.67-01 4.69-01 4.75-01 5.02-01 5.38-01 5.84-01 6.65-01 7.46-01 8.38-01 1.46-01
     7    1 2.95+10 1.83-01 1.85-01 1.86-01 1.90-01 2.02-01 2.18-01 2.36-01 2.67-01 2.98-01 3.34-01 5.92-02
     8    1 0.00+00 5.00-04 5.71-04 5.41-04 6.03-04 1.71-03 2.90-03 3.05-03 2.01-03 1.21-03 6.71-04 0.00+00
     9    1 1.17+10 3.60-02 3.63-02 3.65-02 3.73-02 4.18-02 4.66-02 4.93-02 5.14-02 5.44-02 5.91-02 1.09-02
    10    1 0.00+00 2.39-04 2.39-04 2.40-04 2.90-04 7.15-04 1.05-03 1.02-03 6.62-04 4.23-04 2.70-04 8.92-05
     3    2 0.00+00 2.65-02 3.56-02 4.06-02 4.01-02 3.86-02 3.85-02 3.31-02 2.09-02 1.30-02 7.51-03 0.00+00
     4    2 0.00+00 2.46-02 2.76-02 2.62-02 2.34-02 2.17-02 2.18-02 1.94-02 1.34-02 9.37-03 6.59-03 2.84-03
     5    2 0.00+00 9.04-03 1.12-02 1.05-02 8.66-03 8.79-03 9.92-03 8.83-03 5.35-03 3.13-03 1.71-03 9.60-07
     6    2 0.00+00 9.29-03 7.39-03 5.83-03 4.78-03 5.02-03 5.87-03 5.63-03 3.84-03 2.47-03 1.47-03 0.00+00
     7    2 1.50+10 1.16-01 1.17-01 1.18-01 1.20-01 1.27-01 1.36-01 1.48-01 1.71-01 1.93-01 2.18-01 3.81-02
     8    2 0.00+00 3.32-04 3.42-04 3.28-04 3.38-04 5.59-04 8.13-04 8.36-04 5.65-04 3.51-04 2.01-04 0.00+00
     9    2 1.34+09 5.22-03 5.28-03 5.31-03 5.47-03 6.46-03 7.43-03 7.76-03 7.68-03 7.85-03 8.34-03 1.49-03
    10    2 0.00+00 8.71-05 8.75-05 8.87-05 1.03-04 2.14-04 3.09-04 3.04-04 2.08-04 1.40-04 9.41-05 2.95-05
     4    3 0.00+00 8.39-02 7.78-02 7.19-02 6.50-02 6.29-02 6.53-02 5.90-02 3.96-02 2.57-02 1.59-02 1.97-03
     5    3 0.00+00 1.25-02 1.48-02 1.56-02 1.53-02 1.65-02 1.78-02 1.59-02 1.02-02 6.31-03 3.63-03 0.00+00
     6    3 9.67+09 1.84-01 1.79-01 1.76-01 1.77-01 1.87-01 2.02-01 2.20-01 2.52-01 2.82-01 3.17-01 5.34-02
     7    3 1.17+10 1.00-01 1.01-01 1.02-01 1.03-01 1.10-01 1.19-01 1.29-01 1.46-01 1.62-01 1.81-01 3.12-02
     8    3 5.62+10 1.33-01 1.34-01 1.35-01 1.38-01 1.45-01 1.55-01 1.68-01 1.92-01 2.17-01 2.44-01 4.31-02
     9    3 9.14+08 8.30-03 8.34-03 8.35-03 8.53-03 1.06-02 1.26-02 1.26-02 1.03-02 8.72-03 7.84-03 1.06-03
    10    3 0.00+00 9.78-05 9.84-05 9.93-05 1.28-04 4.12-04 6.77-04 6.76-04 4.26-04 2.51-04 1.37-04 0.00+00
     5    4 0.00+00 2.45-02 3.56-02 4.43-02 4.71-02 4.49-02 4.29-02 3.87-02 3.26-02 2.98-02 2.87-02 2.92-02
     6    4 2.04+09 6.58-02 6.70-02 6.59-02 6.47-02 6.98-02 7.82-02 8.37-02 8.76-02 9.24-02 9.96-02 1.54-02
     7    4 1.73+07 1.46-02 1.91-02 1.84-02 1.57-02 1.55-02 1.75-02 1.65-02 1.12-02 7.31-03 4.59-03 6.20-05
     8    4 0.00+00 4.79-03 5.32-03 5.05-03 4.60-03 5.10-03 6.00-03 5.74-03 3.91-03 2.51-03 1.49-03 0.00+00
     9    4 1.41+11 5.87-01 5.92-01 5.97-01 6.08-01 6.38-01 6.79-01 7.39-01 8.54-01 9.69-01 1.10+00 2.03-01
    10    4 0.00+00 1.04-03 1.05-03 1.05-03 1.12-03 1.65-03 2.10-03 2.07-03 1.61-03 1.31-03 1.13-03 9.49-04
     6    5 0.00+00 5.30-03 5.61-03 4.77-03 3.74-03 3.85-03 4.69-03 4.49-03 2.94-03 1.82-03 1.04-03 0.00+00
     7    5 6.60+08 1.82-02 1.84-02 1.81-02 1.78-02 1.89-02 2.05-02 2.20-02 2.41-02 2.62-02 2.88-02 4.42-03
     8    5 0.00+00 1.84-03 1.87-03 1.76-03 1.64-03 1.75-03 1.90-03 1.74-03 1.20-03 7.91-04 4.83-04 0.00+00
     9    5 1.03+10 7.24-02 7.30-02 7.36-02 7.50-02 7.94-02 8.49-02 9.19-02 1.05-01 1.18-01 1.32-01 2.31-02
    10    5 0.00+00 2.94-04 2.95-04 2.98-04 3.25-04 4.98-04 6.53-04 6.48-04 4.90-04 3.74-04 2.92-04 1.54-04
     7    6 0.00+00 6.00-02 6.06-02 5.87-02 5.83-02 8.23-02 1.04-01 9.90-02 6.98-02 4.97-02 3.63-02 1.91-02
     8    6 0.00+00 1.37-02 1.37-02 1.32-02 1.33-02 2.04-02 2.69-02 2.65-02 1.97-02 1.51-02 1.21-02 8.74-03
     9    6 0.00+00 2.81-02 2.99-02 2.98-02 2.98-02 4.05-02 4.90-02 4.50-02 2.89-02 1.79-02 1.05-02 6.23-04
    10    6 0.00+00 6.75-03 6.74-03 6.69-03 6.87-03 8.77-03 9.96-03 9.06-03 6.05-03 3.92-03 2.36-03 0.00+00
     8    7 0.00+00 2.16-02 2.16-02 2.10-02 2.11-02 2.94-02 3.59-02 3.32-02 2.15-02 1.34-02 7.82-03 0.00+00
     9    7 0.00+00 2.14-02 2.71-02 2.86-02 2.79-02 3.28-02 3.74-02 3.39-02 2.20-02 1.41-02 8.80-03 1.95-03
    10    7 1.12+10 1.82-02 1.83-02 1.85-02 1.88-02 2.07-02 2.24-02 2.31-02 2.35-02 2.43-02 2.60-02 4.61-03
     9    8 0.00+00 6.59-03 6.95-03 6.92-03 6.86-03 8.91-03 1.08-02 1.01-02 6.55-03 4.06-03 2.33-03 0.00+00
    10    8 0.00+00 1.34-03 1.33-03 1.32-03 1.36-03 1.77-03 2.06-03 1.90-03 1.28-03 8.22-04 4.92-04 0.00+00
    10    9 1.47+11 4.39-01 4.43-01 4.47-01 4.55-01 4.78-01 5.09-01 5.54-01 6.42-01 7.28-01 8.22-01 1.42-01
    -1
    -1   -1
```

temperatures and for the allowed transitions where the resonance contributions are less important. The problem with the top-up in the BZ calculations can be seen well in Fig. 8a where the other two results are in almost perfect agreement. The resonance effects can be clearly seen in the forbidden transitions at cooler temperatures where the differences between the various calculations are larger. Finally Fig. 8e is an example in which the level mixing can play a role. Here the amount of mixing of the $2s^2 2p^3 3d\ ^3D_2$ level differs in the current and the Landi & Gu approximations.

4. Summary

We have presented collisional and radiative data for transitions between 342 levels of Fe XIX calculated in the close-coupling approximation using the R-matrix technique. This is the largest close-coupling calculation yet performed for this ion. For the lowest levels, good agreement is found with the previous Iron Project calculation for this ion of Butler & Zeippen (2001) while reasonable agreement is found with the more restricted calculation of McLaughlin et al. (2001) although the latter results tend to underestimate the collision strengths. The agreement with the distorted wave computation of Landi & Gu (2006) is also good at high temperatures with differences being seen at low temperatures due to the more extensive inclusion of resonances in the present work. Larger differences are seen for higher lying levels where level-mixing can become important.

In summary, the collisional data presented in this paper are the best currently available for Fe XIX.

References

Badnell, N. R. 1986, J. Phys. B: At. Mol. Opt. Phys., 19, 3827
Badnell, N. R., & Griffin, D. C. 2001, J. Phys. B: At. Mol. Opt. Phys., 34, 681
Berrington, K. A., Eissner, W. B., & Norrington, P. H. 1995, Comput. Phys. Commun., 92, 290
Bhatia, A. K., Fawcett, B. C., Lemen, J. R., et al. 1989, MNRAS, 240, 421
Butler, K., & Zeippen, C. J. 2001, A&A, 372, 1083
Burgess, A. 1974, J. Phys. B: At. Mol. Opt. Phys., 7, L364
Burgess, A., & Tully, J. A. 1992, A&A, 254, 436
Burke, V. M., Burke, P. G., & Scott, N. S. 1992, Comput. Phys. Commun., 69, 76
Corliss, C., & Sugar, J. 1982, J. Phys. Chem. Ref. Data, 11, 135
Dere, K. P., Landi, E., Mason, H. E., et al. 1997, A&AS, 123, 149
Eissner, W., Jones, M., & Nussbaumer, H. 1974, Comput. Phys. Commun., 8, 270
Griffin, D. C., Badnell, N. R., & Pindzola, M. S. 1998, J. Phys. B: At. Mol. Opt. Phys., 31, 3713
Gu, M. F. 2003, ApJ, 582, 1241
Hummer, D. G., Berrington, K. A., Eissner, W., et al. 1993, A&A, 279, 298
Kotochigova, S., Kirby, K. P., & Tupitsyn, I. 2007, Phys. Rev. A, 76, 052513
Landi, E., & Gu, M. F. 2006, ApJ, 640, 1171
Landi, E., Del Zanna, G., Young, P. R., et al. 2006, ApJS, 162, 261
Loulergue, M., Mason, H. E., Nussbaumer, H., et al. 1985, A&A, 150, 246
McLaughlin, B. M., Kirby, K., Smith, R., et al. 2001, J. Phys. B: At. Mol. Opt. Phys., 34, 4521
Sugar, J., & Corliss, C. 1985, J. Phys. Chem. Ref. Data 14, Suppl., 2, 498
Summers, H. P. 2004, The ADAS User Manual, version 2.6 http://adas.phys.strath.ac.uk
Wang, T. J., Innes, D. E., & Solanki, S. K. 2006, A&A, 455, 1105
Whiteford, A. D., Badnell, N. R., Ballance, C. P., et al. 2001, J. Phys. B: At. Mol. Opt. Phys., 34, 3179
Zhang, H. L., & Sampson, D. H. 2001, ADNDT, 82, 357